Fast coarsening in unstable epitaxy with desorption

P. Šmilauer,[1] M. Rost,[2] and J. Krug[3]

[1]*Institute of Physics, Academy of Sciences of the Czech Republic, Cukrovarnická 10, 162 53 Praha 6, Czech Republic*

[2]*Helsinki Institute of Physics, P.L. 9, 00014 University of Helsinki, Finland*

[3]*Fachbereich Physik, Universität GH Essen, 45117 Essen, Germany*

(Received 19 January 1999)

Homoepitaxial growth is unstable towards the formation of pyramidal mounds when interlayer transport is reduced due to activation barriers to hopping at step edges. Simulations of a lattice model and a continuum equation show that a small amount of desorption dramatically speeds up the coarsening of the mound array, leading to coarsening exponents between 1/3 and 1/2. The underlying mechanism is the faster growth of larger mounds due to their lower evaporation rate. [S1063-651X(99)51006-4]

PACS number(s): 68.55.−a, 05.70.Ln, 68.45.Da, 81.10.Aj

I. INTRODUCTION

Pattern-forming instabilities in homoepitaxial crystal growth, first predicted by Villain [1], have been identified experimentally for a wide range of systems [2–4]. Their ubiquity results from additional activation barriers to hopping at step edges, which reduce interlayer transport and lead to the creation of pyramidal features (*mounds*) on the surface. Much theoretical work in this area has been inspired by a formal analogy with phase ordering kinetics [5–8], aiming in particular at an understanding of the coarsening law $\xi(t) \sim t^{1/z}$ for the increase of the typical mound size ξ with time which is observed in experiments [3,4] and simulations [9,10]. Different universality classes of phase ordering are distinguished, among other things, by the presence or absence of conservation laws for the order parameter and other dynamically relevant fields [11]. In general, conservation laws slow down the dynamics and hence imply smaller values for the coarsening exponent $1/z$.

In this Rapid Communication we discover a similar effect in unstable homoepitaxy: Using kinetic Monte Carlo (KMC) simulations and continuum equations of motion, we show that even a minute amount of desorption drastically changes the coarsening law for the typical mound size. In all previous work desorption was neglected, which implies volume conservation for the growing film [1]. Analytic approaches [6,7] and numerical work [3,7] then suggest the upper bound $1/z \leqslant 1/4$ to hold in the *absence* of in-plane anisotropy, while in the anisotropic case Siegert [12] has recently shown that $1/z \leqslant 1/3$. By contrast, in the presence of desorption we obtain values $1/3 \leqslant 1/z \leqslant 1/2$. For the isotropic continuum equation we find clear evidence for a crossover from $1/z = 1/4$ (the value attained without desorption [3,7]) to $1/z = 1/2$ with increasing film thickness, while for the solid-on-solid KMC model typical values range from $1/z \approx 0.3$ to 0.42, to be compared with $1/z \approx 0.19 - 0.26$ found for the same model in the conservative case [9]. Detailed investigation of the growth kinetics reveals that the mechanism of speedup is a dependence of the evaporation rate on the mound size, leading to faster growth of big mounds at the expense of smaller ones.

II. MONTE CARLO SIMULATIONS

To study epitaxial growth with desorption, we used a solid-on-solid KMC model in which the crystal is assumed to have a simple cubic structure with neither bulk vacancies nor overhangs allowed. The basic processes included in our model are the deposition of atoms onto the surface at a rate F, their surface diffusion, and evaporation from the surface. The diffusion of surface adatoms is modeled as a nearest-neighbor hopping process at the rate $k_D = k_0 \exp(-E_D/k_B T)$, where E_D is the hopping barrier, T is the substrate temperature, and k_B is Boltzmann's constant. The prefactor k_0 is the attempt frequency of a surface adatom and is assigned the value 10^{13} s^{-1}. The barrier to hopping is given by $E_D = E_S + nE_N + (n_i - n_f)\Theta(n_i - n_f)E_B$, where E_S, E_N, and E_B are model parameters, n is the number of in-plane nearest neighbors before the hop, n_i and n_f are the number of next-nearest neighbors in the planes beneath and above the hopping atom before (n_i) and after (n_f) a hop, and $\Theta(x) = 1$ if $x > 0$, and 0 otherwise (cf. Ref. [9] for a more detailed description of the model). The evaporation of a surface adatom occurs at the rate $k_{\rm ev} = k_0 \exp(-E_{\rm ev}/k_B T)$, where $E_{\rm ev} = E_0 + nE_N$ with E_0 being the energy for evaporation of a free surface adatom.

The simulations were carried out on square 300×300 to 600×600 lattices with periodic boundary conditions. The basic set of model parameters and growth conditions used was $E_S = 1.54$ eV, $E_N = 0.23$ eV, $E_B = 0.175$ eV, and $F = 1/6$ monolayer (ML)/s (set I of Ref. [9]). Under these conditions the equilibrium evaporation flux is [13] $F_{\rm eq} = k_0 \exp[-(E_0 + 2E_N)/k_B T)] \approx (10^{-3} - 10^{-2}) \times F$, and the actual desorption rate is a few times larger. The robustness of the observed behavior was tested by using different temperatures and evaporation barriers E_0, and by including the ''incorporation radius'' effect whereby the incoming atom is placed at the site with the highest number of lateral nearest neighbors within a square area of size R_i centered on the site of incidence [9].

Simulation results are shown in Fig. 1 [14]. As the desorption rate increases, coarsening becomes faster and the coarsening exponent $1/z$ becomes much bigger than the range of values observed in previous simulation work using the same model without desorption [9]. Even a rather small amount of desorption [16] thus drastically affects the coarsening exponent regardless of the details of the simulation model (such as the model parameters and the incorporation

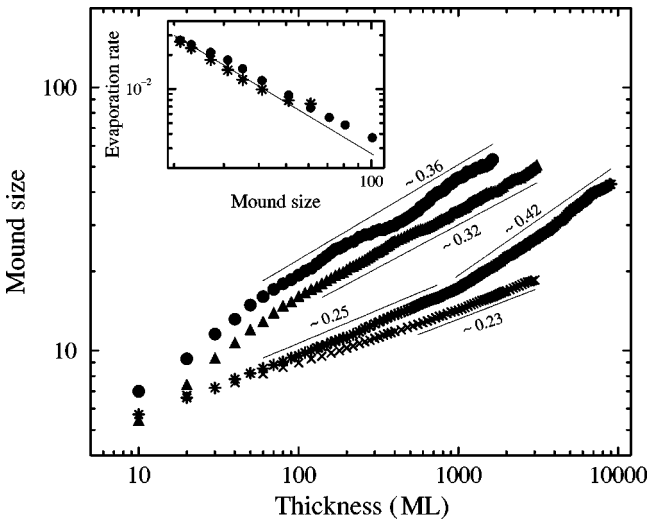

FIG. 1. Lateral mound size $\xi(t)$ evolution for different model parameters and growth conditions obtained in KMC simulations. The model parameters used were $E_0=1.9$ eV at $T=750$ K, $R_i=0$ (stars) and $R_i=3$ (circles), $E_0=2.0$ eV at $T=750$ K, $R_i=3$ (crosses), and $E_0=1.75$ eV at $T=670$ K, $R_i=3$ (triangles). The slopes indicated are the results of least-squares fitting. The error bars of the exponents (estimated from run-to-run variations) are of the order of 0.01. Inset: size-dependent contribution to the evaporation rate of a single mound determined on lattices of size 21, 23, 27, 31, 35, 41, 51, 61, 71, 81, and 101 with periodic boundary conditions. Data show the average over 25 runs, in each of which about 1000 ML were deposited. The full line has the form $\Delta v = A/\xi^{1.5}$, and is consistent with coarsening exponents for the same model parameters.

radius). In the regions of fits shown in Fig. 1 the mound slope stays approximately constant, indicating that the asymptotic regime has been reached. An interesting feature of Fig. 1 is the crossover observed for the case $R_i=0$ after approximately 1000 ML were deposited. We discuss the underlying change in the mechanism of coarsening below.

Figure 2 shows plane and perspective views of the surface morphology after approximately 2000 ML have been deposited. Pyramidal mounds are separated by narrow, deep troughs. The surface profile is clearly asymmetric with flat, rounded mound tops and sharp, deep valleys. For the case of $R_i=3$, mounds are much shallower and bigger, having also more regular structure. In both cases, however, very fast coarsening is observed.

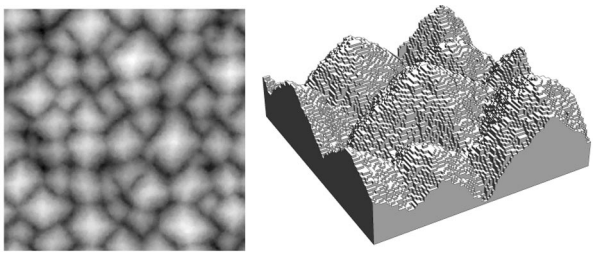

FIG. 2. Surface morphology in KMC simulations after approximately 2000 ML have been deposited. The displayed part of the lattice is 300×300 (plane view, left) and 100×100 (perspective plot, right).

III. CONTINUUM EQUATIONS

Further confirmation of the dramatic effect of evaporation comes from the continuum theory, where the surface is modeled by a smooth, space and time-dependent height function $H(\mathbf{x},t)$. Our starting point is the standard continuum equation for unstable epitaxy [1–3,5–7], to which the leading order effect of desorption is added in terms of a slope-dependent growth rate $V(|\nabla H|)$:

$$\frac{\partial H}{\partial t}=-K\Delta^2 H-\nabla\cdot[f(|\nabla H|^2)\nabla H]+V(|\nabla H|). \quad (1)$$

In the absence of desorption $V(u)\equiv F$, the external flux. For a vicinal surface with step spacing ℓ (tilt $u=a/\ell$, with lattice constant a), the growth rate according to BCF theory reads [17] $V_{\mathrm{BCF}}(\ell)=(Fx_s/\ell)\tanh(\ell/x_s)$ where $x_s=2\sqrt{D\tau}$ is the desorption length, depending on the diffusion coefficient D and the desorption rate $1/\tau$ from a flat surface.

To use the BCF-expression also for near singular surfaces [18], we introduce an effective, tilt-dependent step spacing ℓ_{eff}, which equals ℓ in the step flow regime, $u\gg a/\ell_D$, and reduces to the terrace size or island distance [19] ℓ_D for small u. Desorption is considered a small, perturbative effect in the sense that

$$\alpha\equiv\ell_D/x_s\ll1, \quad (2)$$

which means that it is much more likely for an atom to be captured at a step than to desorb. Under this condition the terrace size ℓ_D should not be influenced by desorption. A plausible formula for ℓ_{eff} is $\ell_{\mathrm{eff}}(u)=\ell_D[1+u^2(\ell_D/a)^2]^{-1/2}$, and the growth rate is then $V(u)=V_{\mathrm{BCF}}[\ell_{\mathrm{eff}}(u)]$. Because of Eq. (2), $\ell_{\mathrm{eff}}(u)\leqslant\ell_D\ll x_s$ for all slopes, and therefore we can expand V_{BCF} to obtain

$$V(u)\approx F\{1-(\alpha^2/3)[1+u^2(\ell_D/a)^2]^{-1}\}. \quad (3)$$

The growth rate varies between $V(0)=F[1-(1/3)\alpha^2]$ for the singular surface and F for $u\gg a/\ell_D$.

In the second term on the right-hand side of Eq. (1) we set $f(u^2)=f_0[1-(u/m_0)^2]$, which leads to a stable selected slope m_0 [5], as is observed in our lattice simulations [20]. We subtract the deposited film thickness, $H\to H-Ft$ and rescale time, lateral space, and height variables to arrive at the dimensionless form [7]

$$\frac{\partial h}{\partial t}=-\Delta^2 h-\nabla\cdot\{[1-(\nabla h)^2]\nabla h\}-\frac{\alpha^2/3}{1+(\nabla h)^2}. \quad (4)$$

The one-dimensional version of Eq. (4) with an evaporation rate $\sim(\nabla h)^2$ was considered in a different context by Emmott and Bray [21].

We integrated Eq. (4) numerically (for the method and system sizes, see [15]) and found similar behavior as in the lattice model. After an initial fast increase of the lateral mound size ξ, the pattern coarsens as in the case without evaporation, $\xi\sim w\sim t^{1/4}$ [3,7] (w is the mean square width of the surface, $w^2=\langle\tilde{h}^2\rangle$ where $\tilde{h}=h-\langle h\rangle$ denotes the height profile relative to its mean). This behavior is transient and eventually crosses over to a fast asymptotic increase of the mound size and the surface width as $\xi\sim w\sim t^{1/2}$. The mound

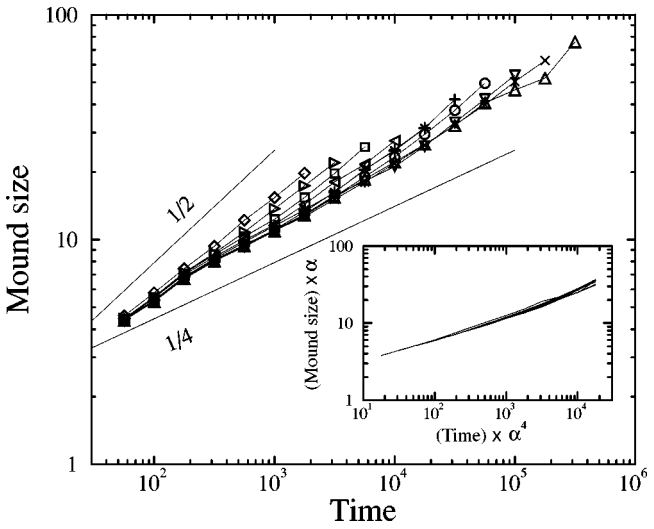

FIG. 3. Lateral mound size $\xi(t)$ for nine different evaporation strengths $\alpha^2/3=10^{-1/2},10^{-5/8},10^{-3/4}, \ldots, 10^{-3/2}$ obtained by numerical integration of the continuum equation. The transient regime $\xi\sim t^{1/4}$ persists until evaporation dominates the surface driven coarsening at $t_\alpha\sim\alpha^{-4}$, the crossover time to asymptotic fast coarsening $\xi\sim t^{1/2}$. The scaling plot in the inset shows time $t\times\alpha^4$ and length $\xi\times\alpha$.

size $\xi(t)$ is shown in Fig. 3 for values of $\alpha^2/3$ ranging from $10^{-1/2}$ to $10^{-3/2}$, decreased by a factor $10^{-1/8}$ between succeeding curves. The transient $t^{1/4}$ regime is absent for the strongest evaporation ($\alpha^2/3=10^{-1/2}$) and becomes more pronounced as α is decreased. A similar crossover is observed in the KMC simulations with $R_i=0$ (stars in Fig. 1).

The evaporation term in Eq. (4) breaks the up-down symmetry ($h\leftrightarrow -h$) [22,25]. When it is dominant (in the fast coarsening regime at late times) the surface morphology is asymmetric. The profile shown in Fig. 4 consists of conical mounds separated by well defined, narrow valleys. Notice that there are no ''negative mounds.'' The grayscale plot shows the cellular arrangement of the cones. The observed features are very similar to results of simulations in Fig. 2.

IV. ORIGIN OF FAST COARSENING

Allowing for evaporation fundamentally changes the nature of the growth instability, because it introduces a coupling between the local growth rate and the surface morphology. In particular, one expects generically a dependence of the average growth rate of a mound on its size, while for conserved growth only the *fluctuations* in the growth rate are size dependent [23]. To see how this can affect the coarsening law, assume that the growth velocity of a mound depends on its size ξ as

$$v(\xi)=v_0-\Delta v(\xi), \tag{5}$$

where $\Delta v(\xi)\sim\xi^{-\nu}$ with a *positive* prefactor, so that large mounds grow faster. If ξ is the only macroscopic length in the system, the size differences between mounds are also of the order of ξ. The time scale on which a small mound is eliminated by its larger neighbors is then given by $t_\xi\sim w/\Delta v(\xi)$, since the surface width w equals the typical height of mounds. Using that the mounds have a constant slope, $w\sim\xi$, it follows that $\xi\sim t^{1/(1+\nu)}$ or $z=1+\nu$. For sufficiently small ν this implies fast coarsening.

A well-known mechanism for a size-dependent growth rate is the Gibbs-Thomson-effect: For spherical droplets in equilibrium the evaporation rate is proportional to the curvature $\sim 1/\xi$, hence within the Wilson-Frenkel-approximation [13] the growth rate is of the form (5) with $\nu=1$. The mounds in our lattice simulations are more conical in shape, with rather straight sides and rounded regions of lateral extent $\approx\ell_D$ at the tips. Assuming that desorption occurs preferentially from the tip regions, the evaporation rate of a mound of size ξ has a contribution proportional to the ratio of the tip area $\sim\ell_D^2$ to the mound area $\sim\xi^2$, leading to $\nu=2$ and $1/z=1/3$. For a more quantitative estimate, $\Delta v(\xi)$ was determined in a sequence of simulations on small square lattices of lateral size 21,23,... up to 101 [24]. As initial configuration on each of them a single mound was prepared. It persisted during deposition of 1000 monolayers, and the average evaporation rate was determined from a sequence of 25 runs. The data presented in Fig. 1 show that $\Delta v(\xi)>0$ and $\nu=1.5\pm 0.1$, which is consistent with direct observations of coarsening on large lattices (cf. Fig. 1).

An analytical evaluation of $\Delta v(\xi)$ is possible for the continuum equation, which will also allow us to derive the scaling of the crossover times (cf. Fig. 3) with α. We recall the surface profile of Fig. 4. The cones show *two* lateral length scales: (i) their size ξ, which for late times is much larger than (ii) ℓ_D, the diameter of the tips and the valleys [$=O(1)$ in our rescaled units], which is independent of ξ.

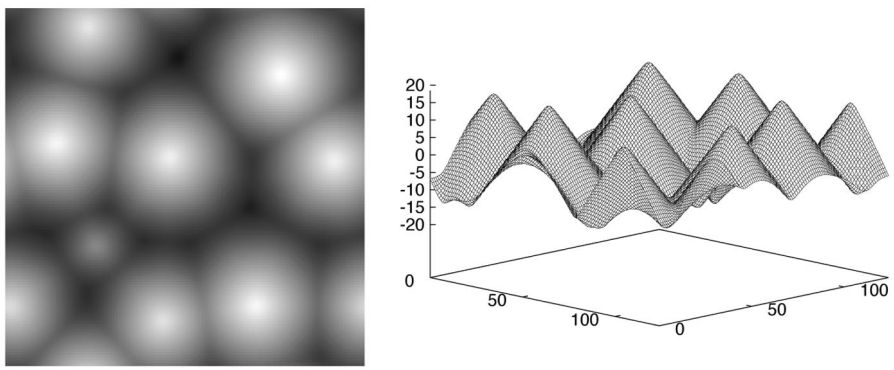

FIG. 4. Surface profile from continuum equation (evaporation $\alpha^2/3=10^{-1/2}$) at late times when $\xi\sim t^{1/2}$. Conical mounds (right) form a cellular structure visible in the gray-scale representation (left).

Thus for a mound on a d-dimensional surface the fraction of the surface covered by the tip is $(1/\xi)^d$. The surrounding trough has codimension one and a relative weight $1/\xi$, while the major part of the surface consists of the sloped sides of the conical mounds.

Evaporation is less pronounced on the mounds' sides whereas it is enhanced by an amount of order α^2 on the horizontal parts, i.e., on the tip and in the surrounding valley. As a consequence Eq. (5) also holds for the continuum equation, where v_0 is the evaporation rate on the mounds' sides, and the enhanced mass loss from small mounds is mainly due to the surrounding valley, i.e., $\Delta v(\xi) \sim \alpha^2/\xi$. So the timescale for mound coalescence is $t_\xi \sim w/\Delta v(\xi) \sim \xi^2/\alpha^2$ (due to the stable slope, $w \sim \xi$), and it follows that $\xi \sim \alpha t^{1/2}$. Incidentally, the same coarsening law was found in the one-dimensional case [21].

The initial increase $\xi \sim t^{1/4}$ is not due to evaporation and thus is the same for all values of α (see Fig. 3). Together with the late time behavior $\xi \sim \alpha t^{1/2}$ this yields the estimate $t_\alpha \sim \alpha^{-4} = (x_s/\ell_D)^4$ for the time at which evaporation begins to dominate the coarsening process. Rescaling time as t/t_α and length as $\xi/t_\alpha^{1/4}$, and omitting the initial fast increase puts all curves and in particular the crossover times t_α on top of each other, as shown in the inset of Fig. 3.

V. DISCUSSION AND CONCLUSION

We emphasize that fast coarsening for the continuum equation is due to the dominance of evaporation from valleys compared to the rest of the mounds. Direct inspection shows that in the KMC simulations more atoms in fact evaporate from the *upper* parts of the mounds. This explains why the coarsening exponent observed for the lattice model is smaller than 1/2: Given enhanced evaporation only on the tips, $\Delta v(\xi)$ is of the order of α^2/ξ^d, leading to $\xi \sim (\alpha^2 t)^{1/(d+1)}$ in d dimensions, hence $z=3$ for $d=2$ as argued previously. To improve on this estimate, more detailed information about the shape of mounds and its coupling to the evaporation rate would be needed. It is nevertheless interesting to note that the coarsening exponent $1/z = 1/(d+1)$ is always larger than the value $1/z = 1/(d+2)$ obtained for noise-induced coarsening [23], indicating that our conclusions will not be modified by shot noise.

In summary, we have identified a general mechanism for fast mound coarsening in unstable growth with desorption. While the detailed appearance of the effect is different in the lattice model as compared to the continuum equation, in both cases the key feature is the dependence of growth rate on mound size. This gives us confidence that the phenomenon is robust and will be observed under suitable experimental conditions.

ACKNOWLEDGMENTS

Support by Volkswagen-Stiftung (P.Š. and J.K.), DFG/SFB 237 (J.K. and M.R.), the Grant Agency of the Czech Republic, Grant No. 202/96/1736 (P.S.), and the COSA program of the Academy of Finland (M.R.) is gratefully acknowledged. P. Castulík provided valuable assistance during the initial stages of this project.

[1] J. Villain, J. Phys. I **1**, 19 (1991).
[2] M.D. Johnson *et al.*, Phys. Rev. Lett. **72**, 116 (1994).
[3] J.A. Stroscio *et al.*, Phys. Rev. Lett. **75**, 4246 (1995).
[4] J.E. Van Nostrand *et al.*, Phys. Rev. Lett. **74**, 1127 (1995); K. Thürmer *et al.*, *ibid.* **75**, 1767 (1995); F. Tsui *et al.*, *ibid.* **76**, 3164 (1996); J.E. Van Nostrand *et al.*, Phys. Rev. B **57**, 12 536 (1998).
[5] M. Siegert and M. Plischke, Phys. Rev. Lett. **73**, 1517 (1994).
[6] L. Golubović, Phys. Rev. Lett. **78**, 90 (1997).
[7] M. Rost and J. Krug, Phys. Rev. E **55**, 3952 (1997).
[8] For reviews see J. Krug, Adv. Phys. **46**, 139 (1997); Physica A **263**, 174 (1999).
[9] P. Šmilauer and D.D. Vvedensky, Phys. Rev. B **52**, 14 263 (1995).
[10] J.G. Amar and F. Family, Phys. Rev. B **54**, 14 742 (1996); K. Thürmer *et al.*, Surf. Sci. **395**, 12 (1998).
[11] A.J. Bray, Adv. Phys. **43**, 357 (1994).
[12] M. Siegert, Phys. Rev. Lett. **81**, 5481 (1998).
[13] J.D. Weeks and G.H. Gilmer, Adv. Chem. Phys. **40**, 157 (1979).
[14] The mound size $\xi(t)$ is measured as the full width at half maximum of the height-height correlation function [15].
[15] M. Rost, P. Šmilauer, and J. Krug, Surf. Sci. **369**, 393 (1996).
[16] For strong desorption, $1/z$ attains values very close to 1/2 and the average mound size saturates after some time.
[17] W.K. Burton, N. Cabrera, and F.C. Frank, Philos. Trans. R. Soc. London, Ser. A **243**, 299 (1951).
[18] A. Pimpinelli and P. Peyla, J. Cryst. Growth **183**, 311 (1998).
[19] J. Villain, A. Pimpinelli, L.-H. Tang, and D.E. Wolf, J. Phys. I **2**, 2107 (1992).
[20] Fast coarsening with desorption does not require the presence of a stable slope m_0. We also observed it for other forms of f introduced in [7], in particular $f(u^2) = f_0/(1+u^{\gamma+1})$ with $\gamma = 1$ and 3.
[21] C.L. Emmott and A.J. Bray, Phys. Rev. E **54**, 4568 (1996).
[22] Conservative terms breaking the up-down symmetry are also expected to be present [3,8]; however, since they do not affect the coarsening law [3,25] they will be ignored here.
[23] L.-H. Tang, P. Šmilauer, and D.D. Vvedensky, Eur. Phys. J. B **2**, 409 (1998).
[24] This is more than the range which is covered by the mound size during our growth simulations.
[25] P. Politi, Phys. Rev. E **58**, 281 (1998).